Molecular and Cellular Biochemistry (2020) 475:63–77
https://doi.org/10.1007/s11010-020-03860-1

Circular RNA hsa_circ_0096157 contributes to cisplatin resistance by proliferation, cell cycle progression, and suppressing apoptosis of non-small-cell lung carcinoma cells

Huasong Lu[1] · Xun Xie[1] · Ke Wang[1] · Quanfang Chen[1] · Shuangqi Cai[1] · Dongmei Liu[1] · Jin Luo[1] · Jinliang Kong[1]

Received: 11 December 2019 / Accepted: 26 July 2020 / Published online: 6 August 2020

Abstract

Circular RNAs (circRNAs) play a major role in cancer development and chemotherapy resistance. This study aimed to characterize circRNA profiles associated with Cisplatin (diamminedichloroplatinum, DDP) resistance of non-small-cell lung carcinoma (NSCLC) cells. The half-maximal inhibitory concentration (IC50) of A549 and A549/DDP cells was determined using CCK-8 assay. Further, circRNA profiles and differentially expressed genes in A549 and A549/DDP cells were characterized by deep sequencing and cell proliferation was measured using MTS assay. Cell cycle progression was analyzed using flow cytometry. Apoptosis experiment was performed by TUNEL assay and flow cytometry. Cell migration and invasion were assessed using the Transwell system. Finally, signalling protein levels related to cell cycle progression and migration were measured by western blot. CCK-8 assay showed that A549/DDP cells obtained strong DDP resistance. Further deep sequencing results showed that 689 circRNAs and 87 circRNAs were significantly upregulated and downregulated in A549/DDP cells compared to A549 cells, respectively. Moreover, the circRNA hsa_circ_0096157 with the highest expression level in A549/DPP cells was further analyzed for its potential mechanism of DDP resistance in A549/DDP. With or without DDP treatment, hsa_circ_0096157 knockdown inhibited proliferation, migration, invasion and cell cycle progression but promoted apoptosis of A549/DDP cells. In addition, the western blot results also showed that hsa_circ_0096157 knockdown in A549/DDP cells increased P21 and E-cadherin but decreased CDK4, Cyclin D1, Bcl-2, N-cadherin, and Vimentin protein expression levels, indicating that cell cycle progression might be inhibited by increased P21 protein level to inhibit the expression of CDK4-cyclin D1 complex and decreased Bcl-2 protein level; and migration and invasion were suppressed by the increased E-cadherin and decreased N-cadherin and Vimentin expression levels. In contrast, hsa_circ_0096157 overexpression in A549 cells caused the opposite cellular and molecular alterations. DDP resistance in NSCLC cells was associated with significant circRNA profile alterations. Moreover, increased hsa_circ_0096157 expression contributed to DDP resistance in NSCLC cells by promoting cell proliferation, migration, invasion and cell cycle progression and inhibiting apoptosis.

Keywords Circular RNA · Cisplatin resistance · Hsa_circ_0096157 · Non-small-cell lung carcinoma · Apoptosis

Introduction

Lung cancer is one of major severe cancers with high incidence and mortality which has been listed as one leading cause of cancer-related deaths worldwide during the past decades [1, 2]. The development of lung cancer is reported to be associated with smoking, exposure to carcinogens, persistent pulmonary inflammation, and also susceptibility

Huasong Lu and Xun Xie are Co-first author.

Huasong Lu and Xun Xie contributed equally to this work.

Electronic supplementary material The online version of this article (https://doi.org/10.1007/s11010-020-03860-1) contains supplementary material, which is available to authorized users.

✉ Jin Luo
66875350@qq.com

✉ Jinliang Kong
kjl071@126.com

[1] Pulmonary and Critical Care Medicine Ward, The First Affiliated Hospital of Guangxi Medical University, No. 6, Shuangyong Road, Qingxiu District, Nanning 530021, Guangxi, People's Republic of China

due to genetic mutations [3–5], however, the molecular pathogenesis underlying lung cancer development is still far from being fully understood. Pathologically, lung cancers are mainly classified into two subtypes including the small-cell lung carcinoma (SCLC) and non-small-cell lung carcinoma (NSCLC) [3]. NSCLC is traditionally termed due to its histological and cytological features significantly different from SCLC, and epidemiology reports show that NSCLC accounts for more than 80% lung cancer cases worldwide [3, 6]. Many chemotherapy drugs such as Cisplatin (diamminedichloroplatinum, DDP) and Vinorelbine are widely applied for NSCLC treatments, however, their efficacy are greatly impaired by the frequent drug resistances which usually lead to poor responses and high recurrence rates [7, 8]. The disclosure of molecular mechanisms underlying chemotherapy resistance are critical for surmounting chemotherapy resistance and developing novel drugs.

The resistance of NSCLC cells to chemotherapies are reported to be a complex cellular processes associated with numerous molecular events [7, 8]. Previous investigations reveal that acquired resistance of NSCLC cells to Cisplatin treatment is caused by the alteration of several DNA repair pathways such as the nucleotide excision repair (NER) pathway and homologous recombination (HR) pathway, which effectively modulate the sensitivity of NSCLC cells to Cisplatin [9]. Moreover, the resistance of NSCLC cell line A549 to Cisplatin treatment has been closely linked with suppressed G2/M cell cycle arrest and apoptosis, caused by altered expression of signaling proteins such as P21, mouse double minute 2 homolog and xeroderma pigmentosum complementation group C [10]. In addition, elevations of the Janus kinase 2 (JAK2) and signal transducers and activators of transcription 3 (STAT3) also contribute to the acquired resistance of A549 to Cisplatin treatment, and inhibition of the JAK/STAT pathway activation is shown to sensitize A549 cells to Cisplatin treatment [11]. The Cisplatin resistance of NSCLC also involves altered expression of many other signaling components such as PI3K/Akt pathway and TGF-β receptor 2 pathway [11, 12]. However, the molecular mechanisms driving the abnormal expressional alterations of these key signaling pathway genes associated with Cisplatin resistance in NSCLC cells remains poorly understood.

Circular RNAs (circRNAs) are a large group of noncoding RNA molecules which are newly characterized to modulate functional gene expression through sponging miRNA and interacting with RNA binding protein [13, 14]. Recent reports have established circRNAs as key regulators of various biological processes and pathogenic conditions such as NSCLC development [15, 16]. For instance, the circRNA hsa_circ_0007385 expression is reported to be significantly elevated in both NSCLC tissue and cell lines, which can act as an novel oncogene during NSCLC development and progression potentially through targeting the miR-181 expression [17]. More importantly, circRNAs are also significantly involved in the acquirement of multiple resistances of cancer cells to chemotherapies [18–20]. Has_circ_0006528 may play a role in breast cancer chemoresistance [18]. Hsa_circ_0000199 originating from the *AKT3* gene enhances the Cisplatin resistance of gastric cancer cells by suppressing miR-198 and promoting PIK3R1 expression [21]. In addition, the high expression of circRNA PVT1 is reported to promote the resistances of osteosarcoma cells to Doxorubicin and Cisplatin treatments by regulating the expression of *ATP-binding cassette subfamily B (ABCB1)* gene [20]. Nevertheless, the expression of circRNAs which might contribute to the Cisplatin resistance of NSCLC cells are still largely unexplored.

In this study, differentially expressed circRNA profiles between NSCLC cell line A549 and its Cisplatin-resistant counterpart A549 DDP were characterized in large scale by deep sequencing. Moreover, the potential roles of hsa_circ_0096157 which was derived from the well-known long noncoding RNA-metastasis-associated lung adenocarcinoma transcript 1 (MALAT1) was further investigated. MALAT1 has been previously established as one essential regulator of Cisplatin resistance in lung cancer cells by modulating cell proliferation, apoptosis and epithelial to mesenchymal transition [21, 22]. The elucidation of circRNA profile alteration and MALAT1-derived hsa_circ_0096157 in this study would provide novel insights into the potential functions of circRNAs in chemotherapy resistance of lung cancers.

Material and methods

Cell culture and reagents

The non-small-cell lung carcinoma A549 (#CC0202) and Cisplatin-resistant A549/DDP cells were purchased from the CELLCOOK company (Guangzhou, China) and cultured in the F12K medium (#N3520; Sigma-Aldrich) supplemented with 2.5 g/L $NaHCO_3$ and 10% fetal bovine serum (FBS; Thermo Fisher Scientific) at 37 °C in a humified culture cabinet with supply of 5% CO_2. A549/DDP cells were cultured in Cisplatin-free F12K medium under normal conditions for one week upon cell recovery, followed by culture in F12K medium containing 1 μg/ml DDP (Sigma) until cell confluency reached 90–95%. After cell passage, A549/DDP cells were first cultured in Cisplatin-free F12K medium until adherent to culture bottle and then maintained in F12K medium containing 2 μg/ml DDP.

CCK-8 and cisplatin IC50 assays

The half-maximal inhibitory concentration (IC50) of Cisplatin in A549 and A549/DDP cells were determined by

measuring the cell viabilities using CCK-8 kit after treatments with 0, 2, 4, 8, 16, 32 and 64 μg/ml DDP for 24 h. The viabilities of A549 and A549/DDP cells were evaluated using the CCK-8 kit (#C0038; Beyotime, Beijing, China) as instructed by the manufacturer. Briefly, NSCLC cells were seeded in 96-well plates and cultured in F12K medium containing DDP at designated concentrations for 24 h, followed by incubation with the CCK-8 reagent for another 24 h at 37 °C. Cell viabilities were finally determined by measuring the absorbance at 450 nm (OD450) on a multiplex plate reader.

CircRNA and mRNA profiling and bioinformatics

To investigate the circRNA profile differences between A549 and A549/DDP cells, the total RNA samples were separately extracted from cultured A549 and A549/DDP cells using TRIzol reagent (Thermo Fishier Scientific; USA) according to the manufacturer's instructions. CircRNAs profiles were sequenced and quantitated as previously introduced with minor modifications [23]. Briefly, RNA samples were first analyzed by the agarose gel electrophoresis and Agilent 2100 Bioanalyzer for determination of RNA integrity and size distribution, followed by removal of rRNA components using the Qiagen RiboMinus Eukayote Kit following the manufacturer's instructions. The resultant RNA samples were then used for construction of RNA library using the NEBNext® Ultra™ II RNA Library Prep Kit (#E7770S; New England Biolabs, Beverly, USA) as instructed by the manufacturer, which were finally sequenced with a Hiseq 2000 system (Illumina, USA).

Clean reads were then subjected to alignment with the reference genome database via the Bowtie2 software [24], and read junctions were selected using the back-splice algorithm. CircRNAs were predicted and annotated with the de novo circRNA identification software CIRI [25]. Relative expressional levels of circRNAs between A549 and A549/DDP cells were assessed by the Mapped backsplicing junction reads per million mapped reads (RPM) through normalization to numbers of total reads. Significantly differentially expressed circRNAs were defined by an FDR (false discovery rate) of ≤ 0.05 and a $\log_2$Ratio of ≥ 1. The differentially expressed mRNAs between A549 and A549/DDP cells were also analyzed by deep sequencing as previously described [26]. The R software package (Version 1.0.8) was used to establish the hierarchical clustering, scatter plot and volcano plot of differentially expressed circRNAs and mRNAs. Gene ontology (GO) categorization of differentially expressed circRNAs were performed using the DAVID (Database for Annotation, Visualization and Integrated Discovery) website. Signaling pathways with significant enrichment of differentially expressed genes were analyzed using the Kyoto Encyclopedia of Genes and Genomes (KEGG) method (https://www.genome.jp/kegg/). The interaction network between circRNAs and mRNAs were established with the cytoscape software (V. 3.2.1).

RT-PCR and quantitative RT-PCR

The circRNAs were confirmed in this study by RT-PCR method using opposite-directed and divergent primers, and differential expressions of circRNAs were validated by quantitative RT-PCR method. Briefly, total RNA samples were extracted from cultured NSCLC cells as introduced above. The cDNA library was established using the Prime Script RT Master Mix kit (#RR036A; Takara) following the manufacturer's instructions. To validate the circular morphology of circRNAs, the divergent and corresponding opposite-directed primer pairs were designed for detection of circRNA and linear genomic DNA, respectively. GAPDH was also detected as the control. For analysis of circRNA expressional levels, the quantitative RT-PCR (qRT-PCR) was performed using the 2 × EasyTaq PCR SuperMix kit (#AS111-03; Transgen Biotech, Beijing, China) according to the manufacturer's instructions. Primers used for PCR in this study were listed in Table 1.

Cell transfection

For knockdown of hsa_circ_0096157 expression in A549/DDP cells, siRNA sense (5′-GAGGGGTGAGGTGGGAGATTA-3′) and antisense (5′-TAATCTCCCACCTCACCCCTC-3′) were synthesized by the GenePharma company (Shanghai, China). Also, the DNA sequences coding the hsa_circ_0096157 were amplified and ligated with the LV003 plasmids for overexpressing hsa_circ_0096157 in A549 cells. NSCLC cells seeded and cultured 6-well plates for 24 h were then transfected with above siRNA sequences or recombinant circRNA-overexpressing plasmids using the Lipofectamine ™ 2000 transfection system (Invitrogen, USA) following the manufacturer's instructions. 48 h after transfection, the expression of hsa_circ_0096157 in NSCLC cells were validated by quantitative RT-PCR method.

Cell proliferation

The proliferation rates of NSCLC cells were analyzed by the MTS method using the CellTiter 96® AQueous Non-Radioactive Cell Proliferation Assay (MTS) (#G5421) provided by the Promega Biotech Co., Ltd. (Beijing) following the manufacturer's instructions. Briefly, NSCLC cells after specified transfections were then seeded in a 96-well plate (100 μl/well). Cells were incubated with 20 μl combined MTS/PMS solution for 2 h at 37 °C. Cell proliferation was finally evaluated by measuring the absorbance at 492 nm (OD492) using a plate reader.

Table 1 Primers used for RT-PCR and qRT-PCR assays

Primer ID	Primer sequences (5′-3′)	Product length (bp)
hsa_circ_0096157-CF1	CACCAGTGGACAAAATGAGGA	172
hsa_circ_0096157-CR1	TAATCTCCCACCTCACCCCT	
hsa_circ_0096157-line-F1	ACACTCAGCAGACACACGTA	117
hsa_circ_0096157-line-R1	TGGTTCCCAATCCCCACATT	
hsa_circ_0030411-CF1	TGCCTAAAAGAGTGAAAAGCCA	190
hsa_circ_0030411-CR1	TCAGTTCTGGTGCCTCTTCA	
hsa_circ_0030411-line-F1	AAGTGTACCTGGGAAGGCTG	165
hsa_circ_0030411-line-R1	TCAGTTCTGGTGCCTCTTCA	
hsa_circ_0005941-CF1	TGGAGGGTGTGATGATCTCA	110
hsa_circ_0005941-CR1	CCAAGGTTCCTGTTGAGCAC	
hsa_circ_0005941-line-F1	GTCGAGTTTGAGTGGCTGAG	90
hsa_circ_0005941-line-R1	CAGTTGAGCCATGGGTTGAC	
hsa_circ_0008865-CF1	ACAGTGAGATAGAGCAGAAAGAG	138
hsa_circ_0008865-CR1	TCATGTCAACTTCAGAAGGCTC	
hsa_circ_0008865-line-F1	TGAGGAGCCTTCTGAGGAAGA	138
hsa_circ_0008865-line-R1	GGGTTACAGTCCGGTTCAGG	
hsa_circ_0012020-CF1	GGTGACATCCTGCAGCTTTT	124
hsa_circ_0012020-CR1	TCTGATGTTCCTGCACCTCA	
hsa_circ_0012020-line-F1	ATCCTTCGGCTCAGTGGAAA	175
hsa_circ_0012020-line-R1	AGGGAAGGAATGTAACGGCA	
hsa_circ_0006157-CF1	TCTGTGAACTAGCTTCTTTGTGA	152
hsa_circ_0006157-CR1	TGGATGAGATATCGAAGCGCT	
hsa_circ_0006157-line-F1	AGAGGACACAAGCACTTCGA	140
hsa_circ_0006157-line-R1	AATGCATGCTCGGACCATTC	
GAPDH -CF1	TCCTCACAGTTGCCATGTAGACCC	220
GAPDH -CR1	TGCGGGCTCAATTTATAGAAACCGGG	
GAPDH-line-F1	GAGTCAACGGATTTGGTCGT	185
GAPDH-line-R1	GACAAGCTTCCCGTTCTCAG	

Cell migration and invasion

The Transwell systems (Corning) were used to detect the migration and invasion capacities of NSCLC cells. Briefly, NSCLC cells cultured in serum-free F12K medium were seeded in the upper chamber of Transwell system, of which the lower chamber were filled with F12K medium containing 10% FBS. After culture under normal conditions for 24 h, NSCLC cell migrated into the lower chambers were then stained with crystal violet and observed for assessment of NSCLC cell migration capacity. For analysis of cell invasion, NSCLC cells cultured in serum-free medium were loaded in upper chamber of Transwell system with Matrigel-loaded inner sides. Cells invaded into the lower chambers 24 h later were counted for evaluation of cell invasion capacity. Image J software was used for semi-quantitative analysis of the cell number of migration and invasion.

Cell cycle progression

The progression of cell cycle in NSCLC cells after transfection were determined by flow cytometry combined with Propidium Iodide Flow Cytometry Kit (#ab139418; Abcam). Briefly, NSCLC cells were washed 5 min with PBS for three times, harvested by centrifuge at 1000×*g* for 10 min and then fixed with 70% ethanol for 24 h at 4 °C. After incubation with 200 µl 1X Propidium Iodide (PI) + RNase Staining Solution at 37 °C in darkness for 30 min, the cell cycle progression of NSCLC cells was finally quantitated by flow cytometry.

Cell apoptosis

The apoptosis of NSCLC cells was quantitatively analyzed by flow cytometry (#V13242; Thermo Fishier Scientific) using the Dead Cell Apoptosis Kit with Annexin V-FITC

and PI following the manufacturer's instructions. Briefly, NSCLC cells were washed with PBS, resuspended in cells in 1X Annexin-binding buffer and then incubated with 5 µl Annexin V-FITC and 1 µl 100 µg/ml PI working solution for 15 min at room temperature. The percentages of apoptotic NSCLC cells were finally measured by a flow cytometer. While, TUNEL assay also was performed for cell death detection following the manufacturer's instructions [27]. Apoptosis stained sections were examined by a fluorescence microscope (Carl Zeiss, Tokyo, Japan), and images of 5 random and non-overlapping fields were examined at an objective magnification of × 200 for analysis.

Western blot

Total proteins were extracted from NSCLC cells using the Western and IP Cell Lysis Buffer (#P0013J; Beyotime, Beijing, China) as instructed by the manufacturer. Approximate 30 µg protein were boiled at 100 °C for 5 min, separated by SDS-PAGE and transferred onto PVDF membrane (Millipore, USA). After being blocked with 5% lipid-free milk for 2 h at room temperature, the PVDF membranes were then incubated with primary anti-P21 (#ab218311; dilution 1:1000; Abcam), anti-CDK4 (#12,790; dilution 1:1000; CST), anti-Cyclin D1 (#55,506; dilution 1:1000; CST), anti-Bcl-2 (#ab32124; dilution 1:1000; Abcam), anti-E-cadherin (#3195; dilution 1:1000; CST), anti-N-cadherin (#13,116; dilution 1:1000; CST), anti-Vimentin (#6260; dilution 1:1000; Santa), and anti-GAPDH (#ab181602; dilution 1:1000; Abcam) at room temperature for 2 h, then the membranes were incubated with the appropriate horseradish peroxidase-conjugated secondary antibody (Santa Cruz Biotechnology) for 1 h at room temperature. The immune blots were finally developed with enhanced ECL substrates (Thermo Fishier Scientific). GAPDH was detected as the internal standard.

Statistical analysis

Quantitative data from at least three biological replicates were presented as mean ± standard deviation and analyzed by the SPSS 20.0 software. Significant differences were evaluated by the Student's *t* test and ANOVA as appropriate. The significant differences were defined by a *P* value of < 0.05.

Results

Large-scale identification of circRNAs in A549 and A549/DDP cells

To investigate the circRNAs associated with Cisplatin resistance in NSCLC cells, we first confirmed the resistance of A549/DDP cells by measuring the IC50 of Cisplatin in both cultured A549 and A549/DDP cells. We found through CCK-8 assay that the IC50 of Cisplatin in A549/DDP cells was approximately 16 µg/ml, which was greatly higher than the IC50 of about 4 µg/ml of Cisplatin in A549 cells, showing the A549/DDP cells used in our study possessed high resistance to Cisplatin treatment (Fig. 1a). Subsequently, the circRNA profiles in both the A549 and A549/DDP cells were characterized by next-generation RNA sequencing (Fig. 1b–e). We observed that most circRNAs were identified with 1 to 100 backspliced reads (Fig. 1b). The lengths of identified circRNAs ranged between 1 to 3000 bp, and the majority of circRNAs possessed a length of about 400 bp (Fig. 1c). In addition, our deep sequencing analysis showed that circRNAs identified in NSCLC cells were distributed in almost every human chromosome, and the chromosomes #1 and #2 encoded the largest numbers of circRNAs identified in both the A549 and A549/DDP cells (Fig. 1d). Totally 7137 and 3700 circRNAs were identified in A549 and A549/DDP cells, respectively, and 2286 circRNAs were identified in both the A549 and A549/DDP cells which accounted for 26.7% of all 8551 circRNAs (Fig. 1e). The significantly different circRNA profiles between A549 and A549/DDP cells indicated the critical roles of circRNAs in development of Cisplatin resistance in NSCLC cells.

Differentially expressed circRNAs between A549 and A549/DDP cells

For more insights into the involvement of circRNAs in NSCLC Cisplatin resistance, the expressional alteration of circRNAs between A549 and A549/DDP cells were also quantitatively analyzed during deep sequencing. Using FDR ≤ 0.05 and $\log_2$Ratio ≥ 1 as the threshold, we found that totally 776 circRNAs showed significantly differential expression between the A549 and A549/DDP cells, including 689 up-regulated and 87 down-regulated circRNAs in A549/DDP cells compared with A549 cells (Fig. 2a–c; Supplemental Table 1). The hierarchical clustering (Fig. 2a), scatter plot (Fig. 2b), and volcano plot (Fig. 2c) of these differentially expressed circRNAs clearly demonstrated the significantly distinct circRNA profiles

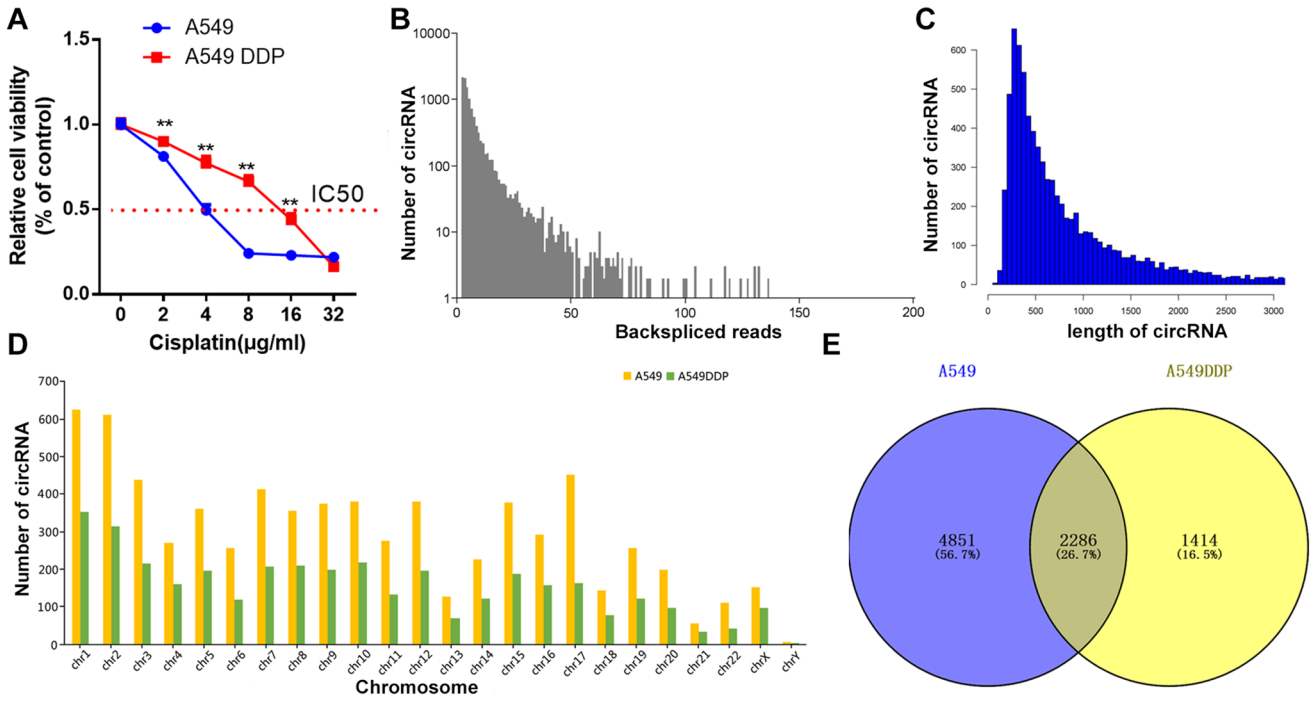

Fig. 1 Large-scale circRNA profiles in A549 and A549/DDP cells by deep sequencing. **a** The IC50 values of A549 and A549/DDP cells determined by CCK-8 method. A549 and A549/DDP cells were separately treated with 0, 2, 4, 8, 16 and 32 μg/ml Cisplatin for 24 h, followed by cell viability analysis via CCK-8 assay. **b** The numbers of backspliced reads of circRNAs identified in A549 and A549/DDP cells by next-generation RNA sequencing. **c** The length distributions of circRNAs identified in A549 and A549/DDP cells via RNA sequencing. **d** Genomic distribution of circRNAs identified between A549 and A549/DDP cells. The circRNAs identified in A549 and A549/DDP cells were indicated in yellow and green bars, respectively. **e** A Venn diagram showing the total numbers of circRNAs identified in A549 and A549/DDP cells. DDP: Cisplatin; IC50: half-maximal inhibitory concentration; $^{**}P < 0.01$

in A549/DDP cells in comparison to A549 cells. Moreover, the expression levels of six identified circRNAs in this study, which were encoded by genes highly expressed in lung cancer or reportedly associated with lung cancer resistance to Cisplatin, were further validated by quantitative RT-PCR method (Fig. 2d). We found that the expression of hsa_circ_0096157 and hsa_circ_0030411 were significantly elevated in A549/DDP cells compared with the A549 cells, while the expression of hsa_circ_0005941 was then suppressed in A549/DDP cells (Fig. 2d). Significantly differential expression of circRNAs in A549/DDP cells compared with A549 cells further supported the roles of circRNAs in resistance of NSCLC cells to Cisplatin treatment. Specifically, the expression of hsa_circ_0096157 showed a 2.5-fold increase in A549/DDP cells (Fig. 2d). The circular morphology of hsa_circ_0096157 was also confirmed by agarose gel electrophoresis using divergent and opposite-directed primer pairs and hsa_circ_0096157 cleavage sites was also verified by Sanger sequencing (Fig. 2e). Therefore, hsa_circ_0096157 was selected for further functional investigations in following assays.

Differential gene expression profiles between A549 and A549/DDP cells

To explore the potential biological processes and signaling pathways possibly regulated by circRNA during Cisplatin resistance development, we further analyzed the gene expression profile alterations between A549 and A549/DDP cells also by next-generation sequencing. Totally, we found the mRNA levels of 859 genes were significantly up-regulated and 1038 genes were down-regulated in A549/DDP cells compared with the A549 cells, using FDR ≤ 0.001 and $\log_2$Ratio ≥ 1 as the threshold (Fig. 3a–c; Supplemental Table 2). Through GO categorization, we found that these genes differentially expressed in A549 and A549/DDP cells were significantly enriched in various biological processes, such as cellular response to stimulus, cell communication, cell differentiation and proliferation, programmed cell death, cell adhesion, cell migration, and cell cycle (Fig. 3d).

Moreover, our KEGG pathway analysis showed that these significantly differentially expressed genes between A549 and A549/DDP cells were significantly enriched in

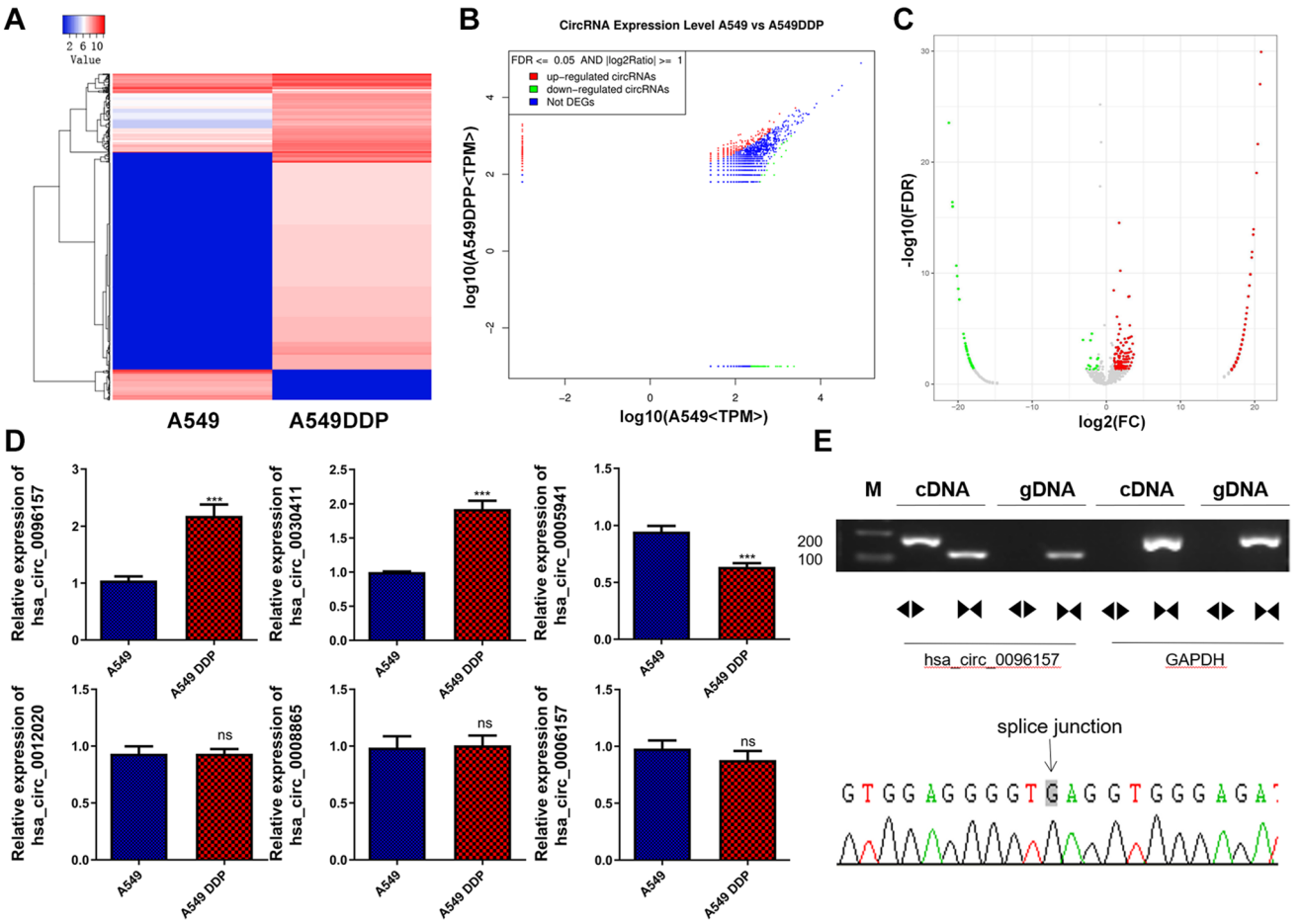

Fig. 2 Significantly differential circRNA profiles between A549 and A549/DDP cells by deep sequencing. **a** The hierarchical clustering of differentially expressed circRNAs between the A549 and A549/DDP cells. Totally 689 up-regulated and 87 down-regulated circRNAs in A549/DDP cells in comparison with A549 cells were used for hierarchical clustering. **b**, **c** The scatter plot (**b**) and volcano plot (**c**) showing the expression of 689 up-regulated and 87 down-regulated circRNAs in A549/DDP cells. **d** The expressional levels of six representative circRNAs between the A549 and A549/DDP cells. Quantitative RT-PCR was performed to analyze the expression of circRNAs in A549 and A549/DDP cells. GAPDH was used as the internal standard. **e** Circular morphology for hsa_circ_0096157 in A549 cells was validated by agarose gel electrophoresis using divergent and opposite-directed primer pairs. Confirmation of splice junction underlying hsa_circ_0096157 by Sanger sequencing. *DDP* Cisplatin; *MALAT1* metastasis-associated lung adenocarcinoma transcript 1, *M* marker, *cDNA* circular DNA, *gDNA* genomic DNA, *ns* not significant; ***$P < 0.001$

many signaling pathways reportedly involved in Cisplatin resistance, including the PI3K/Akt, MAPK, Focal adhesion, TNF, Ras and the Wnt signaling pathways (Fig. 3e). In addition, our bioinformatics analysis revealed an extensive interaction networks between differentially expressed circRNAs and functional proteins associated with cell cycle progression and apoptosis (Supplemental Fig. 1). The large number of genes differentially expressed and its potential interaction with key functional proteins in A549/DDP cells further indicated that the acquirement of Cisplatin resistance in NSCLC cells involved alterations of various biological processes and signaling pathways, which might be modulated by above-characterized differentially expressed circRNAs.

Hsa_circ_0096157 knockdown repressed proliferation and cell cycle progression and promoted apoptosis of A549/DDP cells under Cisplatin treatment and non-treatment

To study the potential functions of hsa_circ_0096157 in Cisplatin resistance of NSCLC cells, we knocked down the expression of hsa_circ_0096157 in A549/DDP cells by transfection with specific siRNAs (Fig. 4a). Quantitative RT-PCR results showed that the expression of has_circ_0096157 was significantly downregulated in siRNA group compared to siNC group (Fig. 4a). Compared with non-Cisplatin treatment, Cisplatin treatment suppressed significantly the proliferation rates of A549/

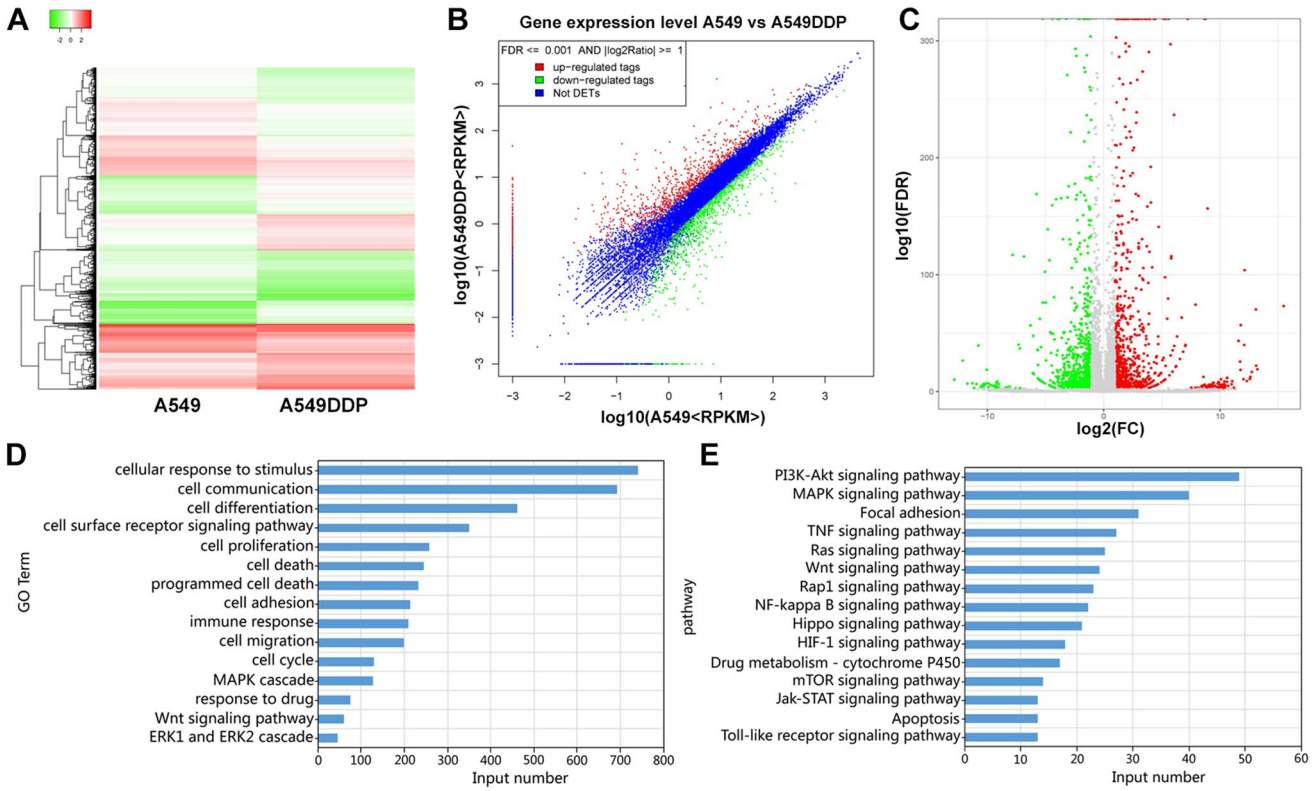

Fig. 3 Differential gene expressional profiles in A549 and A549/DDP cells. **a** A hierarchical clustering of differentially expressed mRNAs between A549 and A549/DDP cells. Totally 859 up-regulated and 1028 down-regulated mRNAs in A549/DDP cells were characterized by deep sequencing compared with A549 cells. **b**, **c** A scatter plot (**b**) and volcano plot (**c**) representing the up-regulation of 689 mRNAs and down-regulation of 1038 mRNAs in A549/DDP cells. **d** Categorization of differentially expressed mRNAs in A549/DDP cells by GO biological processes. **e** The KEGG pathways with significant enrichments of differentially expressed mRNAs in A549/DDP cells. *DDP* Cisplatin, *GO* gene ontology, *KEGG* Kyoto encyclopedia of genes and genomes

DDP cells (Fig. 4b). Interfering with the expression of has_circ_0096157 inhibited significantly the proliferation rates of A549/DDP cells under Cisplatin treatment and non-treatment (Fig. 4b). TUNEL and flow cytometry assays results showed that, compared with non-Cisplatin treatment, Cisplatin treatment promoted significantly the apoptosis of A549/DDP cells (Fig. 4c, d). Interfering with the expression of has_circ_0096157 promoted significantly the apoptosis of A549/DDP cells under Cisplatin treatment and non-treatment (Fig. 4c, d). On the contrary, compared with non-Cisplatin treatment, the flow cytometry results showed that Cisplatin treatment significantly blocked the cell cycle in G1 phase (Fig. 4e). Interfering with the expression of hsa_circ_0096157 significantly blocked the cell cycle in S phase and reduced G2 phase under Cisplatin treatment and non-treatment (Fig. 4e). These results clearly showed that hsa_circ_0096157 knockdown could effectively impair the proliferation and cell cycle progression of A549/DDP cells, however, promote apoptosis of A549/DDP cells under Cisplatin treatment.

Hsa_circ_0096157 promoted proliferation and cell cycle progression and suppressed apoptosis of A549 cells under Cisplatin treatment and non-treatments

For further validation of hsa_circ_0096157 in Cisplatin resistance in NSCLC, the hsa_circ_0096157 was then overexpressed in A549 cells by transfection with the LV003-hsa_circ_0096157 recombinant plasmids (Fig. 5a). Quantitative RT-PCR results showed that the expression of has_circ_0096157 was significantly upregulated in has_circ_0096157 group compared to LV003 group (Fig. 5a). Compared with non-Cisplatin treatment, Cisplatin treatment suppressed significantly the proliferation rates of A549 cells (Fig. 5b). Overexpression of has_circ_0096157 promoted significantly the proliferation rates of A549 cells under Cisplatin treatment and non-treatment (Fig. 5b). TUNEL and flow cytometry assays results showed that, compared with non-Cisplatin treatment, Cisplatin treatment promoted significantly the apoptosis of A549 cells (Fig. 5c, d). Overexpression of has_circ_0096157 inhibited significantly the apoptosis of A549 cells under Cisplatin

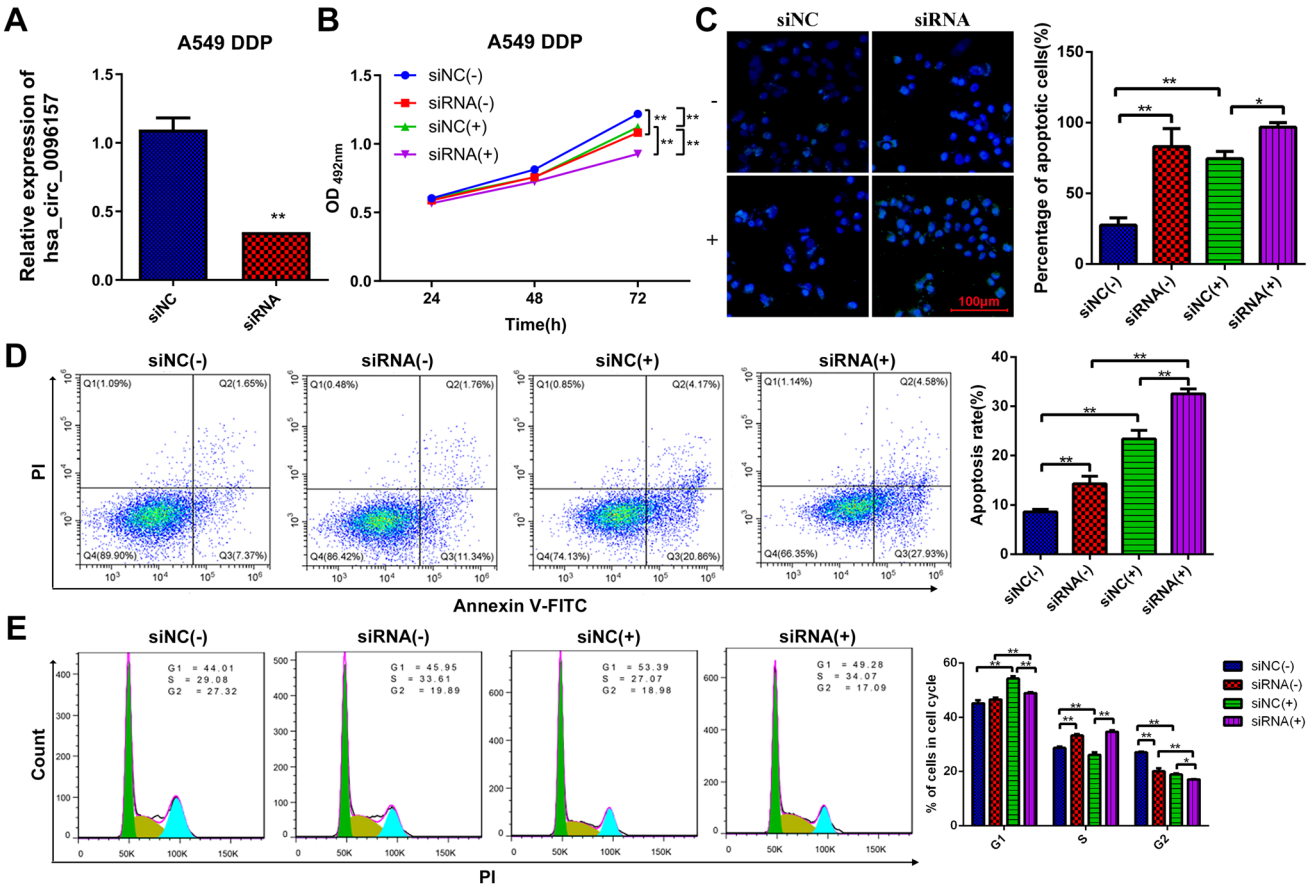

Fig. 4 Regulation of A549/DDP cell proliferation, apoptosis, and cycle progression by hsa_circ_0096157 knockdown under Cisplatin treatment and non-treatment. **a** Significant decrease of hsa_circ_0096157 expression in A549/DDP cells by transfection with siRNAs. Hsa_circ_0096157 expression was assessed by quantitative RT-PCR method. **b** The proliferation rates of A549/DDP cells with or without hsa_circ_0096157 knockdown under Cisplatin treatment and non-treatment. A549/DDP cells were treated with 3 μg/ml DDP for 24 h, and the proliferation was analyzed by MTS method. **c**, **d** The apoptosis of A549/DDP cells with or without hsa_circ_0096157 knockdown under Cisplatin treatment and non-treatment via TUNEL assay (**c**) and flow cytometry (**d**). Percentages of apoptotic A549/DDP cells were determined by Image J software and flow cytometry. **e** The cell cycle progression of A549/DDP cells with or without hsa_circ_0096157 knockdown under Cisplatin treatment and non-treatment. The percentages of A549/DDP cells at G1, S and G2 phases were quantitated by flow cytometry after treatment with 3 μg/ml DDP for 24 h. *DDP* Cisplatin, *NC* negative control, (−) no Cisplatin treatment, (+) treatment with 3 μg/ml Cisplatin for 24 h; $*P<0.05$; $**P<0.01$; $***P<0.001$; bar indicates 100 μm

treatment and non-treatment (Fig. 5c, d). Moreover, compared with non-Cisplatin treatment, the flow cytometry results showed that Cisplatin treatment significantly blocked the cell cycle in G1 phase (Fig. 5e). Overexpression of hsa_circ_0096157 significantly promoted the conversion from S phase to G2 phase under Cisplatin treatment and non-treatment (Fig. 5e). Together, we proved here by these assays that hsa_circ_0096157 overexpression promoted the proliferation and cell cycle progression, however suppressed the apoptosis of A549 cells. More importantly, hsa_circ_0096157 overexpression inhibited the suppression of A549 cell proliferation and cell cycle progression as well as the inducement of A549 cell apoptosis caused by Cisplatin treatment.

Hsa_circ_0096157 knockdown repressed migration and invasion in A549/DDP cells and promoted the migration and invasion in A549 cells

Based on the above effects of circRNA on cell proliferation, cell cycle progression, and apoptosis, we further analyzed the effects of hsa_circ_0096157 knockdown in A549/DDP cells and hsa_circ_0096157 overexpression in A549 cells on cell migration and invasion. The results showed that hsa_circ_0096157 knockdown resulted into significantly suppressed migration and invasion capacities in A549/DDP cells treated with Cisplatin or no Cisplatin (Fig. 6a, b). While hsa_circ_0096157 overexpression resulted into significantly promoted migration and invasion capacities in

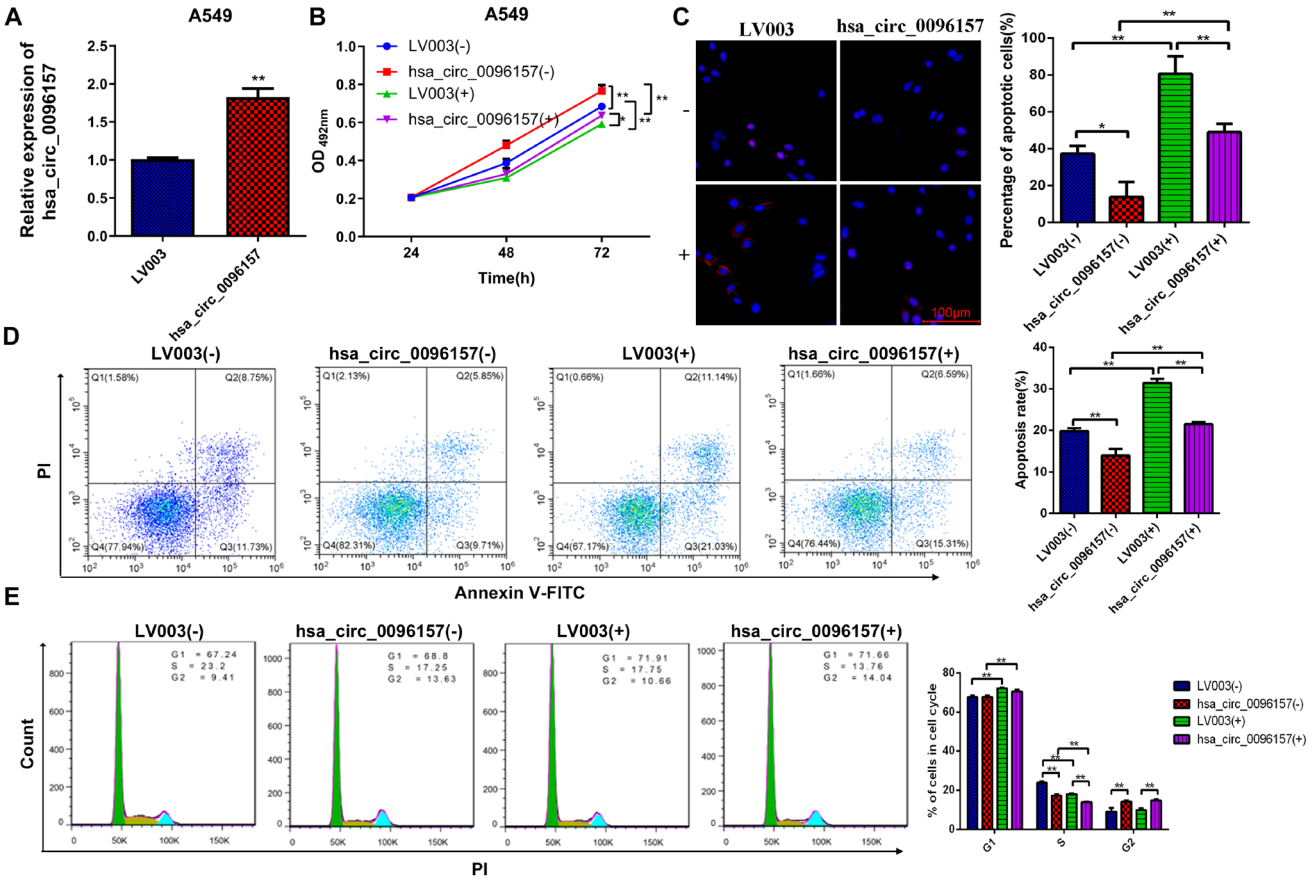

Fig. 5 Modulation of A549 cell proliferation, apoptosis, and cycle progression by hsa_circ_0096157 overexpression under Cisplatin treatment and non-treatment. **a** The increase of hsa_circ_0096157 expression in A549 cells by transfection with overexpressing plasmids. The hsa_circ_0096157 expression was measured by quantitative RT-PCR assay. **b** The changes of proliferation rates in A549 cells overexpressing hsa_circ_0096157 under Cisplatin treatment and non-treatment. After being treated with with 3 μg/ml DDP for 24 h, the proliferation of A549 cells was determined by the MTS method. **c**, **d** The numbers of apoptotic A549 cells with hsa_circ_0096157 overexpression under Cisplatin treatment and non-treatment via TUNEL assay (**c**) and flow cytometry (**d**). The number of apoptotic A549 cells were determined by Image J software and flow cytometry. **e** The alterations of A549 cell cycle progression induced by hsa_circ_0096157 overexpression under Cisplatin treatment and non-treatment. Flow cytometry was performed to analyze the percentages of A549 cells at the G1, S and G2 stages. *DDP* Cisplatin, (−) no Cisplatin treatment, (+) treatment with 3 μg/ml Cisplatin for 24 h; $*P<0.05$; $**P<0.01$; bar indicates 100 μm

A549 cells treated with Cisplatin or no Cisplatin (Fig. 6c, d). Together, the above results indicated that hsa_circ_0096157 knockdown and overexpression played an important role in the migration and invasion of A549/DDP and A549 cells respectively.

Regulation of cell cycle signaling pathway and epithelial-mesenchymal transition (EMT) by hsa_circ_0096157 in A549 and A549/DDP cells

To investigate the molecular events underlying the regulation of Cisplatin resistance by hsa_circ_0096157 in NSCLC, the expression levels of several key components of the cell cycle signaling pathway were quantitatively analyzed in A549 cells overexpressing hsa_circ_0096157 and A549/DDP cells with hsa_circ_0096157 knockdown. We observed that the abundance of P21 and E-cadherin proteins in A549 cells were significantly down-regulated by hsa_circ_0096157 overexpression, however P21 and E-cadherin protein levels in A549/DDP cells were greatly elevated by hsa_circ_0096157 knockdown (Fig. 7a and b). Contrarily, the abundance of CDK4 protein in hsa_circ_0096157-overexpressing A549 cells was significantly higher than the A549 cells, but its level in A549/DDP cells with hsa_circ_0096157 knockdown was markedly lower than the A549/DDP cells (Fig. 7a and b). Furthermore, the protein levels of Cyclin D1, Bcl-2, N-cadherin, and Vimentin showed similar alterations as CDK4 in A549 and A549/DDP cells induced by hsa_circ_0096157 overexpression and knockdown, respectively (Fig. 7a and b), indicating that cell cycle progression might be inhibited by increased P21 protein level to inhibit the expression of CDK4-Cyclin D1 complex and

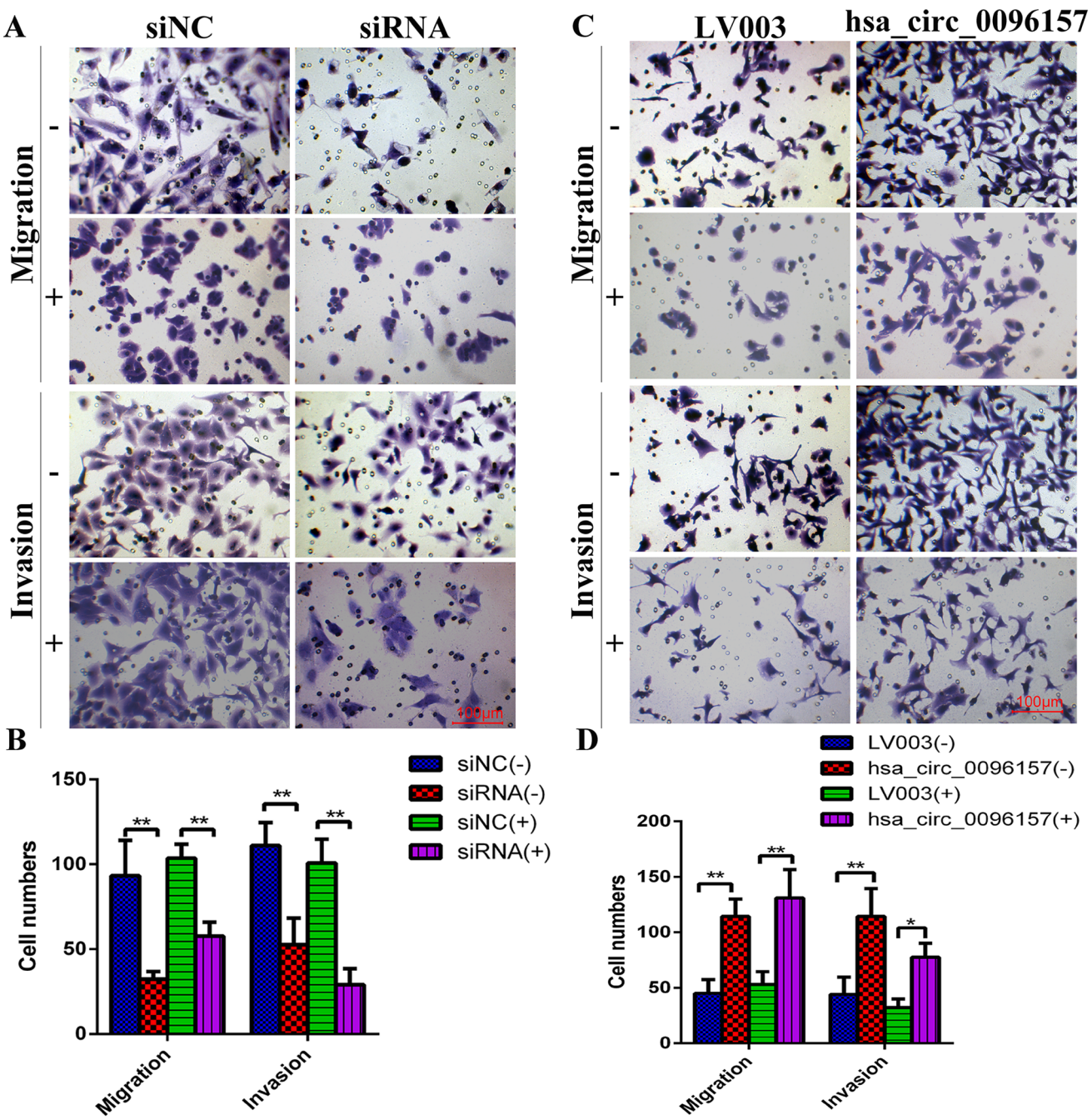

Fig. 6 Migration and invasion analysis of A549/DPP cell with hsa_circ_0096157 knockdown and A549 cell with hsa_circ_0096157 overexpression under Cisplatin treatment and non-treatment. **a** Regulation of A549/DPP cell migration and invasion by hsa_circ_0096157 knockdown. Migration and invasion of A549/DDP cells were analyzed using the Transwell system. **b** Semiquantitative analysis of the number of migration and invasion cells in graph A. **c** Regulation of A549 cell migration and invasion by hsa_circ_0096157 overexpression. Migration and invasion of A549/DDP cells were analyzed using the Transwell system. **d** Semiquantitative analysis of the number of migration and invasion cells in graph C. *DDP* Cisplatin, *NC* negative control; (−) no Cisplatin treatment, (+) treatment with 3 μg/ml Cisplatin for 24 h; $*P<0.05$; $**P<0.01$; bars indicate 100 μm

decreased Bcl-2 protein level; and migration and invasion were suppressed by the increased E-cadherin and decreased N-cadherin and Vimentin expression levels through the hsa_circ_0096157 knockdown in A549/DDP cells. These molecular evidences further verified the regulation of cell cycle signaling pathway and EMT by hsa_circ_0096157 expression alteration, which mediated the acquirement of Cisplatin resistance in NSCLC cells.

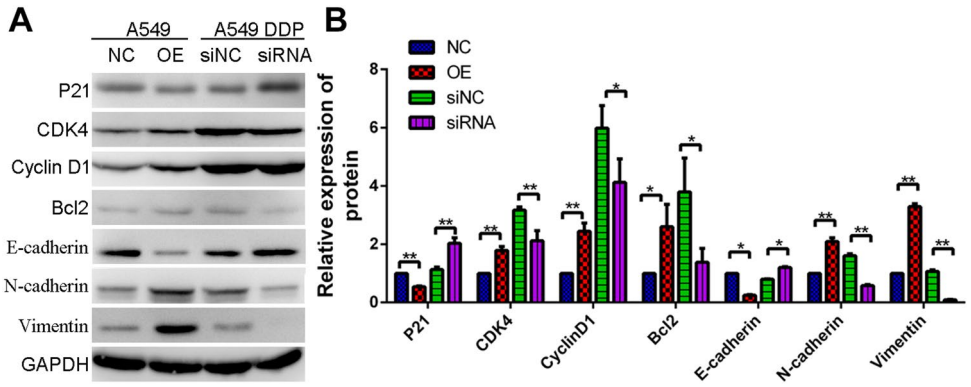

Fig. 7 Changes of the cell cycle signaling pathway and EMT marker in A549 and A549/DDP cells by hsa_circ_0096157. **a** Abundances of key protein components of the cell cycle signaling pathway in A549 cells with hsa_circ_0096157 overexpression and A549/DDP cells with hsa_circ_0096157 knockdown. Protein levels of P21, CDK4, Cyclin D1, Bcl-2, E-cadherin, N-cadherin, and Vimentin in A549 and A549/DDP were measured by western blotting. GAPDH was used as the internal standard. **b** Quantitation of P21, CDK4, Cyclin D1, Bcl-2, E-cadherin, N-cadherin, and Vimentin protein levels in A549 and A549/DDP cells. *DDP* Cisplatin, *NC* negative control, *OE* overexpression; $*P<0.05$; $**P<0.01$

Discussion

The resistance of chemotherapy drugs such as Cisplatin to the treatment of NSCLC has become a huge challenge for cancerous treatment [7, 8]. The full elucidation of the molecular mechanisms underlying acquirement of Cisplatin treatment has been regarded as one essential basis for developing novel treatments for patients resistant to Cisplatin treatment. To provide novel insights into the epigenetic regulation of Cisplatin resistance in NSCLC, we performed a large-scale identification of circRNA profiles in A549 cells and A549/DDP cells with strong resistance to Cisplatin treatment via next-generation deep sequencing method. Totally 7137 and 3700 circRNAs were sequenced in A549 and A549/DDP cells, respectively, among which 776 circRNAs were significantly differentially expressed in A549/DDP cells compared with A549 cells. In consistence with the alteration of circRNA profiles, we also revealed a number of differentially expressed genes in A549/DDP cells associated with various biological processes and signaling pathways linked with cancer development and chemotherapy resistance. Furthermore, we also showed that the proliferation, migration, invasion, cell cycle progression, and apoptosis of A549 and A549/DDP cells were greatly altered by hsa_circ_0096157 knockdown or overexpression under Cisplatin treatment. These assays revealed great changes of circRNA profiles associated with Cisplatin resistance in NSCLC, and proved the hsa_circ_0096157 expression elevation as a driving actor for Cisplatin resistance in NSCLC cells.

Noncoding RNA molecules such as miRNAs and long non-coding RNAs (lncRNAs) have recently been established as essential parts of cellular epigenetic networks, which play critical roles in chemotherapy resistance in NSCLC [26, 28, 29]. For instance, the miR106a expression is greatly upregulated in DDP-resistant A549 cell line, which is reported to confer Cisplatin resistance in A549 cells by modulating the expression of ABCA1, a member of the adenosine triphosphatase binding cassette family [29]. It has been demonstrated by accumulating evidences that circRNAs serve as sponges of miRNAs in various biological and pathogenic processes, resulting into the substantial expressional alterations of key functional genes [30, 31]. However, the circRNAs which may be critically involved in Cisplatin resistance of NSCLC cells remains largely unexplored. The rapid development of next-generation RNA sequencing and combined computational database and analysis tools greatly facilitate identification and annotation of circRNA profiles under distinct contexts [32]. In the present study, we identified a great number of differentially expressed circRNAs in A549/DDP cells and these circRNAs were mainly distributed on chromosomes #1 and #2, indicating the significances of circRNA expression alterations on chromosomes #1 and #2 in Cisplatin resistance. Of note, these 689 upregulated circRNAs in A549/DDP cells greatly overnumbered those 87 down-regulated circRNAs, indicating circRNA expression elevation might serve as a common mechanism promoting NSCLC resistance to Cisplatin treatment. Combined with the great alterations of gene expression profiles revealed in this study, further functional investigation of differentially expression circRNAs and their regulatory networks would put new perspectives on epigenetic regulation of Cisplatin resistance acquirement.

Among the large set of up-regulated circRNAs in A549/DDP cells, we validated by quantitative RT-PCR that hsa_circ_0096157, hsa_circ_0030411, and hsa_circ_0005941 expression levels exhibited significant increase in A549/DDP cells. Previous reports showed hsa_circ_0096157 is formed by the ligation of long noncoding RNA MALAT1,

which is implicated in cell proliferation and apoptosis regulation underlying the resistance of lung cancer to Cisplatin [21, 22]. Alpha-ketoglutarate dependent dioxygenase (FTO) knockdown also inhibited the colony formation ability of lung cancer cells [32], and it can be interfered that has_circ_0005941 derived from *FTO* gene may play an important role in A549/DDP resistance to cisplatin. To explore its biological functions during Cisplatin resistance in NSCLC, we silenced the highest expression level of hsa_circ_0096157 in A549/DDP cells, which resulted into greatly suppressed proliferation, migration, invasion, and cell cycle progression in A549/DDP cells, even under Cisplatin treatment. Previous reports already showed that Cisplatin-resistant NSCLC cells are featured by enhanced proliferation, migration, invasion, and cell cycle progression [33–35]. Also, the abrogation of proliferation and apoptosis alterations in Cisplatin-resistant NSCLC cells has been regarded as a promising strategy to overcoming the resistance of cancer cells to Cisplatin treatment [36, 37]. The effective modulations of A549/DDP cell proliferation and apoptosis as well as other cellular tumorigenesis-related processes by hsa_circ_0096157 knockdown hopefully suggested that targeting hsa_circ_0096157 expression might be utilized as a new method to increase Cisplatin sensitivity and overcome NSCLC resistance to Cisplatin. In consistence, the overexpression of hsa_circ_0096157 in A547 cells in this study produced completely opposite alterations of these cellular processes in A547 cells, which further validated the potential roles of hsa_circ_0096157 in development of Cisplatin resistance in NSCLC cells. These observations also disclosed new mechanisms mediating the tumorigenesis-regulating roles of MALAT1 and other long non-coding RNAs.

It has been well-documented that activation of cell cycle progression substantially promotes the development of Cisplatin in various human cancers [10, 37]. In NSCLC cells, the therapeutic effects of Cisplatin treatment has been partially attributed to its capacity of inducing G2/M cell cycle arrest in cancerous cells, while the development of Cisplatin resistance is mediated by the abrogation of G2/M cell cycle arrest during Cisplatin treatment [10]. In this study, we convincingly demonstrated that the cell cycle progression of A549/DDP cells could be significantly inhibited by hsa_circ_0096157 knockdown under Cisplatin treatment. On the contrary, hsa_circ_0096157 overexpression mitigated the Cisplatin-induced A549 cell cycle arrest. These results further highlighted the significance of cell cycle progression alteration during development of Cisplatin resistance in NSCLC cells. In consistence, we detected consistent alteration of four key signaling proteins regulating cell cycle progression in A549 and A549/DDP cells with altered hsa_circ_0096157 expression. The P21 protein is a well-known tumor suppressor protein which induces cell cycle arrest to inhibit tumorigenesis [38]. Also, the CDK4/Cyclin D1 axis and Bcl-2 protein act as essential checkpoint mechanism and regulatory signaling pathways driving cell cycle progression [39]. We also investigated the expression of EMT biomarkers such as E-cadherin, N-cadherin, and Vimentin, which were involved in the regulation of molecular mechanisms of tumor migration and invasion. Research reveals that overexpression of lncRNA H19 reduces the level of E-cadherin and increases the expression levels of Vimentin and N-cadherin to promoting the A549 cells invasion and metastasis [40]. While, our results also showed that E-cadherin protein level was greatly elevated and Vimentin and N-cadherin protein levels were downregulated in A549/DDP cells by hsa_circ_0096157 knockdown. The corresponding changes of these proteins in NSCLC cells by alteration of hsa_circ_0096157 further indicated the mediating roles of cell cycle regulation and migration in Cisplatin resistance of NSCLC, which deserve further investigations.

In summary, we characterized a large set of significantly differentially expressed circRNA profiles between A549 and A549/DDP cells through next-generation deep sequencing. Moreover, we disclosed for the first time that the elevated expression of hsa_circ_0096157 contributed to Cisplatin resistance by promoting proliferation, migration, invasion, and cell cycle progression; and suppressing apoptosis of NSCLC cells. These results provided novel insights into the noncoding RNAs-mediated Cisplatin resistances and a basis for developing novel treatments for Cisplatin-resistant lung cancer patients.

Author contributions This study concept and design, and the manuscript revision were performed by JL and JK. The experiments performance, data analysis and the manuscript draft were performed by HL and XX. The study design, study implementation and manuscript revision were performed by KW, QC, SC and DL. All authors read and approved the final manuscript.

Funding This work was supported by the National Natural Science Foundation of China (Nos. 81760419 and 81760743) and Beijing Medical and Health Public Welfare Fund Medical Science Research Fund (No. B20151DS).

Compliance with ethical standards

Conflict of interest All authors declare that they have no conflict of interest.

Research involving human participants and/or animals This article does not contain any studies with human participants or animals performed by any of the authors.

References

1. Chen W, Zheng R, Baade PD, Zhang S, Zeng H, Bray F, Jemal A, Yu XQ, He J (2016) Cancer statistics in China, 2015. CA Cancer J Clin 66(2):115–132. https://doi.org/10.3322/caac.21338

2. Siegel RL, Miller KD, Jemal A (2016) Cancer statistics, 2016. CA Cancer J Clin 66(1):7–30. https://doi.org/10.3322/caac.21332
3. Brandao GD, Brega EF, Spatz A (2012) The role of molecular pathology in non-small-cell lung carcinoma-now and in the future. Curr Oncol (Toronto, Ont) 19(Suppl 1):S24–32. https://doi.org/10.3747/co.19.1058
4. Gabrielson E (2006) Worldwide trends in lung cancer pathology. Respirology (Carlton, Vic) 11(5):533–538. https://doi.org/10.1111/j.1440-1843.2006.00909.x
5. Malinovsky G, Yarmoshenko I, Zhukovsky M (2018) Radon, smoking and HPV as lung cancer risk factors in ecological studies. Int J Radiat Biol 94(1):62–69. https://doi.org/10.1080/09553002.2018.1399225
6. Fujimoto J, Wistuba II (2014) Current concepts on the molecular pathology of non-small cell lung carcinoma. Semin Diagn Pathol 31(4):306–313. https://doi.org/10.1053/j.semdp.2014.06.008
7. Fadejeva I, Olschewski H, Hrzenjak A (2017) MicroRNAs as regulators of cisplatin-resistance in non-small cell lung carcinomas. Oncotarget 8(70):115754–115773. https://doi.org/10.18632/oncotarget.22975
8. MacDonagh L, Gray SG, Breen E, Cuffe S, Finn SP, O'Byrne KJ, Barr MP (2018) BBI608 inhibits cancer stemness and reverses cisplatin resistance in NSCLC. Cancer Lett 428:117–126. https://doi.org/10.1016/j.canlet.2018.04.008
9. Chen P, Li J, Chen YC, Qian H, Chen YJ, Su JY, Wu M, Lan T (2016) The functional status of DNA repair pathways determines the sensitization effect to cisplatin in non-small cell lung cancer cells. Cell Oncol (Dordrecht) 39(6):511–522. https://doi.org/10.1007/s13402-016-0291-7
10. Sarin N, Engel F, Kalayda GV, Mannewitz M, Cinatl J Jr, Rothweiler F, Michaelis M, Saafan H, Ritter CA, Jaehde U, Frötschl R (2017) Cisplatin resistance in non-small cell lung cancer cells is associated with an abrogation of cisplatin-induced G2/M cell cycle arrest. PLoS ONE 12(7):e0181081. https://doi.org/10.1371/journal.pone.0181081
11. Jiang Z, Yin J, Fu W, Mo Y, Pan Y, Dai L, Huang H, Li S, Zhao J (2014) MiRNA 17 family regulates cisplatin-resistant and metastasis by targeting TGFbetaR2 in NSCLC. PLoS ONE 9(4):e94639. https://doi.org/10.1371/journal.pone.0094639
12. Sun DM, Tang BF, Li ZX, Guo HB, Cheng JL, Song PP, Zhao X (2018) MiR-29c reduces the cisplatin resistance of non-small cell lung cancer cells by negatively regulating the PI3K/Akt pathway. Sci Rep 8(1):8007. https://doi.org/10.1038/s41598-018-26381-w
13. Jeck WR, Sharpless NE (2014) Detecting and characterizing circular RNAs. Nat Biotechnol 32(5):453–461. https://doi.org/10.1038/nbt.2890
14. Memczak S, Jens M, Elefsinioti A, Torti F, Krueger J, Rybak A, Maier L, Mackowiak SD, Gregersen LH, Munschauer M, Loewer A, Ziebold U, Landthaler M, Kocks C, le Noble F, Rajewsky N (2013) Circular RNAs are a large class of animal RNAs with regulatory potency. Nature 495(7441):333–338. https://doi.org/10.1038/nature11928
15. Hansen TB, Kjems J, Damgaard CK (2013) Circular RNA and miR-7 in cancer. Can Res 73(18):5609–5612. https://doi.org/10.1158/0008-5472.can-13-1568
16. Li Y, Zheng Q, Bao C, Li S, Guo W, Zhao J, Chen D, Gu J, He X, Huang S (2015) Circular RNA is enriched and stable in exosomes: a promising biomarker for cancer diagnosis. Cell Res 25(8):981–984. https://doi.org/10.1038/cr.2015.82
17. Jiang MM, Mai ZT, Wan SZ, Chi YM, Zhang X, Sun BH, Di QG (2018) Microarray profiles reveal that circular RNA hsa_circ_0007385 functions as an oncogene in non-small cell lung cancer tumorigenesis. J Cancer Res Clin Oncol 144(4):667–674. https://doi.org/10.1007/s00432-017-2576-2
18. Gao D, Zhang X, Liu B, Meng D, Fang K, Guo Z, Li L (2017) Screening circular RNA related to chemotherapeutic resistance in breast cancer. Epigenomics 9(9):1175–1188. https://doi.org/10.2217/epi-2017-0055
19. Huang X, Li Z, Zhang Q, Wang W, Li B, Wang L, Xu Z, Zeng A, Zhang X, Zhang X, He Z, Li Q, Sun G, Wang S, Li Q, Wang L, Zhang L, Xu H, Xu Z (2019) Circular RNA AKT3 upregulates PIK3R1 to enhance cisplatin resistance in gastric cancer via miR-198 suppression. Mol Cancer 18(1):71. https://doi.org/10.1186/s12943-019-0969-3
20. Kun-Peng Z, Xiao-Long M, Chun-Lin Z (2018) Overexpressed circPVT1, a potential new circular RNA biomarker, contributes to doxorubicin and cisplatin resistance of osteosarcoma cells by regulating ABCB1. Int J Biol Sci 14(3):321–330. https://doi.org/10.7150/ijbs.24360
21. Cui Y, Li G, Zhang X, Dai F, Zhang R (2018) Increased MALAT1 expression contributes to cisplatin resistance in non-small cell lung cancer. Oncol Lett 16(4):4821–4828. https://doi.org/10.3892/ol.2018.9293
22. Fang Z, Chen W, Yuan Z, Liu X, Jiang H (2018) LncRNA-MALAT1 contributes to the cisplatin-resistance of lung cancer by upregulating MRP1 and MDR1 via STAT3 activation. Biomed Pharmacother 101:536–542. https://doi.org/10.1016/j.biopha.2018.02.130
23. Liu C, Zhang C, Yang J, Geng X, Du H, Ji X, Zhao H (2017) Screening circular RNA expression patterns following focal cerebral ischemia in mice. Oncotarget 8(49):86535–86547. https://doi.org/10.18632/oncotarget.21238
24. Langmead B, Salzberg SL (2012) Fast gapped-read alignment with Bowtie 2. Nat Methods 9(4):357–359. https://doi.org/10.1038/nmeth.1923
25. Yan N, Xu H, Zhang J, Xu L, Zhang Y, Zhang L, Xu Y, Zhang F (2017) Circular RNA profile indicates circular RNA VRK1 is negatively related with breast cancer stem cells. Oncotarget 8(56):95704–95718. https://doi.org/10.18632/oncotarget.21183
26. Brennan EP, Morine MJ, Walsh DW, Roxburgh SA, Lindenmeyer MT, Brazil DP, Gaora P, Roche HM, Sadlier DM, Cohen CD, Godson C (1822) Martin F (2012) Next-generation sequencing identifies TGF-β1-associated gene expression profiles in renal epithelial cells reiterated in human diabetic nephropathy. Biochem Biophys Acta 4:589–599. https://doi.org/10.1016/j.bbadis.2012.01.008
27. Gao Y, Wang J, Zhao F (2015) CIRI: an efficient and unbiased algorithm for de novo circular RNA identification. Genome Biol 16(1):4. https://doi.org/10.1186/s13059-014-0571-3
28. Dong Z, Zhong Z, Yang L, Wang S, Gong Z (2014) MicroRNA-31 inhibits cisplatin-induced apoptosis in non-small cell lung cancer cells by regulating the drug transporter ABCB9. Cancer Lett 343(2):249–257. https://doi.org/10.1016/j.canlet.2013.09.034
29. Ma Y, Li X, Cheng S, Wei W, Li Y (2015) MicroRNA-106a confers cisplatin resistance in non-small cell lung cancer A549 cells by targeting adenosine triphosphatase-binding cassette A1. Mol Med Rep 11(1):625–632. https://doi.org/10.3892/mmr.2014.2688
30. Han D, Li J, Wang H, Su X, Hou J, Gu Y, Qian C, Lin Y, Liu X, Huang M, Li N, Zhou W, Yu Y, Cao X (2017) Circular RNA circMTO1 acts as the sponge of microRNA-9 to suppress hepatocellular carcinoma progression. Hepatology (Baltimore, MD) 66(4):1151–1164. https://doi.org/10.1002/hep.29270
31. Zhang XQ, Yang JH (2018) Discovering circRNA-microRNA Interactions from CLIP-Seq Data. Methods Mol Biol (Clifton, NJ) 1724:193–207. https://doi.org/10.1007/978-1-4939-7562-4_16
32. Saleembhasha A, Mishra S (2018) Novel molecules lncRNAs, tRFs and circRNAs deciphered from next-generation sequencing/RNA sequencing: computational databases and tools. Briefings Funct Genomics 17(1):15–25. https://doi.org/10.1093/bfgp/elx013
33. Ye LY, Hu S, Xu HE, Xu RR, Kong H, Zeng XN, Xie WP, Wang H (2017) The effect of tetrandrine combined with cisplatin on

proliferation and apoptosis of A549/DDP cells and A549 cells. Cancer Cell Int 17:40. https://doi.org/10.1186/s12935-017-0410-1
34. Zhu X, Li D, Yu F, Jia C, Xie J, Ma Y, Fan S, Cai H, Luo Q, Lv Z, Fan L (2016) miR-194 inhibits the proliferation, invasion, migration, and enhances the chemosensitivity of non-small cell lung cancer cells by targeting forkhead box A1 protein. Oncotarget 7(11):13139–13152. https://doi.org/10.18632/oncotarget.7545
35. Cetintas VB, Kucukaslan AS, Kosova B, Tetik A, Selvi N, Cok G, Gunduz C, Eroglu Z (2012) Cisplatin resistance induced by decreased apoptotic activity in non-small-cell lung cancer cell lines. Cell Biol Int 36(3):261–265. https://doi.org/10.1042/cbi20110329
36. Nascimento AV, Singh A, Bousbaa H, Ferreira D, Sarmento B, Amiji MM (2017) Overcoming cisplatin resistance in non-small cell lung cancer with Mad2 silencing siRNA delivered systemically using EGFR-targeted chitosan nanoparticles. Acta Biomater 47:71–80. https://doi.org/10.1016/j.actbio.2016.09.045
37. Zhang Y, Wang X, Han L, Zhou Y, Sun S (2015) Green tea polyphenol EGCG reverse cisplatin resistance of A549/DDP cell line through candidate genes demethylation. Biomed Pharmacother 69:285–290. https://doi.org/10.1016/j.biopha.2014.12.016
38. Tanaka T, Iino M (2014) Knockdown of Sec8 promotes cell-cycle arrest at G1/S phase by inducing p21 via control of FOXO proteins. FEBS J 281(4):1068–1084. https://doi.org/10.1111/febs.12669
39. Shirali S, Aghaei M, Shabani M, Fathi M, Sohrabi M, Moeinifard M (2013) Adenosine induces cell cycle arrest and apoptosis via cyclinD1/Cdk4 and Bcl-2/Bax pathways in human ovarian cancer cell line OVCAR-3. Tumour Biol 34(2):1085–1095. https://doi.org/10.1007/s13277-013-0650-1
40. Liao S, Yu C, Liu H, Zhang C, Li Y, Zhong X (2019) Long non-coding RNA H19 promotes the proliferation and invasion of lung cancer cells and regulates the expression of E-cadherin, N-cadherin, and vimentin. Oncotargets Ther 12:4099–4107. https://doi.org/10.2147/ott.s185156